Shubnikov–de Haas oscillations in bulk $ZrTe_5$ single crystals: Evidence for a weak topological insulator

Yang-Yang Lv,[1] Bin-Bin Zhang,[1] Xiao Li,[2] Kai-Wen Zhang,[2] Xiang-Bing Li,[2] Shu-Hua Yao,[1,*] Y. B. Chen,[2,†] Jian Zhou,[1] Shan-Tao Zhang,[1] Ming-Hui Lu,[1] Shao-Chun Li,[2,3,‡] and Yan-Feng Chen[1,3]

[1]*National Laboratory of Solid State Microstructures & Department of Materials Science and Engineering, Nanjing University, Nanjing 210093, China*

[2]*National Laboratory of Solid State Microstructures & Department of Physics, Nanjing University, Nanjing 210093, China*

[3]*Collaborative Innovation Center of Advanced Microstructure, Nanjing University, Nanjing 210093, China*

(Received 20 December 2015; revised manuscript received 17 March 2016; published 19 March 2018)

The study of $ZrTe_5$ crystals is revived because of the recent theoretical prediction of topological phase in bulk $ZrTe_5$. However, the current conclusions for the topological character of bulk $ZrTe_5$ are quite contradictory. To resolve this puzzle, we here identify the Berry phase on both *b*- and *c* planes of high-quality $ZrTe_5$ crystals by the Shubnikov–de-Hass (SdH) oscillation under tilted magnetic field at 2 K. The angle-dependent SdH oscillation frequency, both on *b*- and *c* planes of $ZrTe_5$, demonstrates the two-dimensional feature. However, phase analysis of SdH verifies that a nontrivial π-Berry phase is observed in the *c*-plane SdH oscillation, but not in the *b*-plane one. Compared to bulk Fermi surface predicted by the first-principle calculation, the two-dimensional-like behavior of SdH oscillation measured at *b* plane comes from the bulk electron. Based on these analyses, it is suggested that bulk $ZrTe_5$ at low temperature ($\sim$2 K) belongs to a weak topological insulator, rather than Dirac semimetal or strong topological insulator as reported previously.

DOI: 10.1103/PhysRevB.97.115137

I. INTRODUCTION

The theoretical prediction and experimental realization of quantum spin Hall effect (QSHE) is one of the greatest progresses achieved in condensed matter physics recently [1–4]. Up to now, the experimental systems to realize the QSHE are semiconductor heterostructures. To relax the stringent requirements to synthesize semiconductor heterostructures, several natural materials hosting QSHE are theoretically predicted [5–7]. Recently, Weng *et al.* proposed that there is QSHE state in the monolayer $ZrTe_5$ [7]. In addition, they also predicted that stacking monolayer $ZrTe_5$ to bulk gives rise to a strong/weak topological insulator (TI), as well as topological phase transition under the mechanical stress/temperature stimuli. This theoretical prediction leads to the revived study of $ZrTe_5$ crystals that have been explored 30 years ago [8–12]. So far, many experimental works have been carried out to clarify topological character of bulk $ZrTe_5$ by different methods and made the contradicting conclusions. For example, Li *et al.* reported that bulk $ZrTe_5$ belongs to a Dirac semimetal and converts to a Weyl semimetal under the magnetic-field by discovering the chiral magnetic effect together with angle-resolved photoemission spectroscopy (ARPES) results [13]. The same conclusion has been reached by Wang *et al.*, who characterized the infrared reflectivity of $ZrTe_5$ with/without magnetic field [14,15]. Using SdH oscillations under high magnetic field ($\sim$31 T), Zheng *et al.* suggested the possibility of $ZrTe_5$ being a 3D Dirac semimetal [16]. The group of Xiu *et al.* also claimed the observation of hallmarks of Dirac fermions by SdH oscillation [17,18]. Different from these works, strong topological insulator is also reported. Manzoni *et al.* used ARPES on (010) surface of $ZrTe_5$ to identify both a surface and a bulk state, which suggests the strong TI character of $ZrTe_5$ [19]. However, some other experiments support that $ZrTe_5$ is a 3D weak TI. For example, Li *et al.* observed a bulk band gap of about 80 meV with topological edge states at the step edge of $ZrTe_5$ by scanning tunneling microscopy [20]. A similar conclusion is also reported by Wu *et al.* [21]. Studying the evolution of the band structure of $ZrTe_5$ at different temperatures and surface doping by ARPES, Moreschini *et al.* showed the edge states in $ZrTe_5$ and no surface states existing at the (010) surface, which is in agreement with features of weak TI [22]. Xiong *et al.* performed a systematic high-momentum-resolution ARPES on $ZrTe_5$ and concluded that $ZrTe_5$ is a 3D weak TI [23]. Similar characterization has been conducted by Zhang *et al.*, who observed quasi-1D electronic features associated with the edge states and the persistence of band gap [24]. Obviously, the topological character of bulk $ZrTe_5$ is still elusive at the current stage.

To solve the above-mentioned puzzles, we grew high-quality $ZrTe_5$ crystals and characterized magnetoresistance of $ZrTe_5$ crystals under tilted magnetic fields B at 2 K. The oscillations up to eighth order can be observed on SdH oscillation of both *b*- and *c*-plane $ZrTe_5$ under maximum $B\sim 9$ T. Angle-dependent SdH quantum oscillation and phase extraction through a Landau fan diagram are studied. Through Berry phase analysis, we conclude that bulk $ZrTe_5$ belongs to a weak topological insulator rather than a 3D Dirac semimetal or a strong topological insulator.

*shyao@nju.edu.cn
†ybchen@nju.edu.cn
‡scli@nju.edu.cn

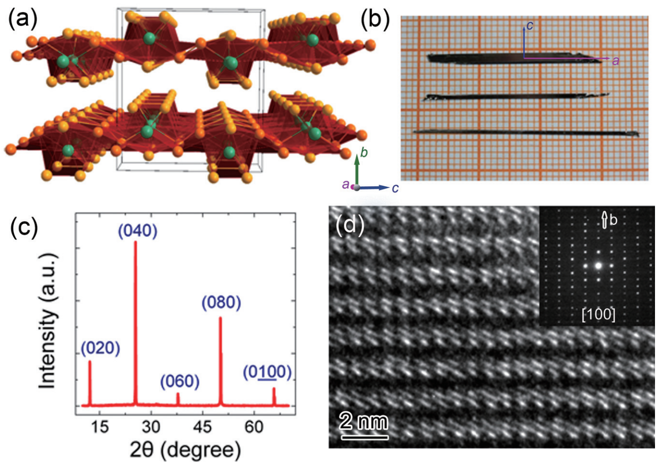

FIG. 1. (a) Schematic of the crystal structure of $ZrTe_5$. (b) Optical micrograph of the grown $ZrTe_5$ single crystals. (c) X-ray diffraction of $ZrTe_5$ crystal sample is indexed with (0 k 0) reflection. (d) and its inset are the high-resolution TEM image of $ZrTe_5$ and corresponding electron diffraction pattern along the [100]-direction, respectively.

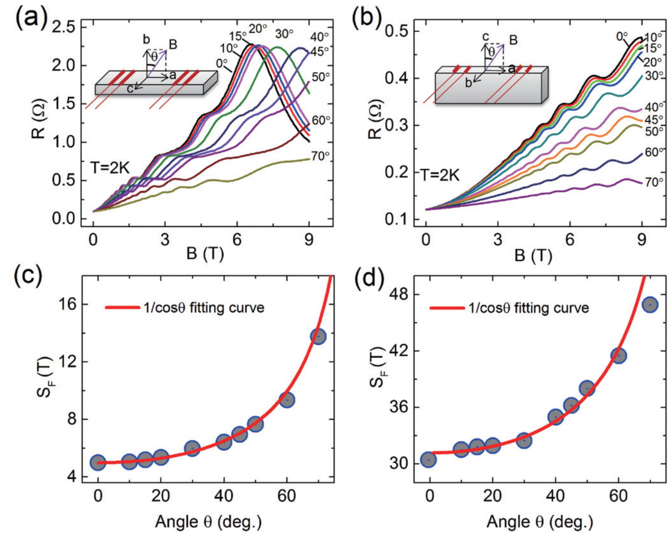

FIG. 2. (a) R_{xx} vs B on b plane with magnetic field B tilted from b- to a axis measured at 2 K. Upper inset is the schematic of the experiment. (b) R_{xx} vs B on c plane with B tilted from c- to a axis measured at 2 K. Upper inset is the schematic of the experiment. (c) Tilting-angle dependent oscillation frequency extracted from the FFT analysis of curves in (a). The red curve is the $1/\cos\theta$ fitting. (d) Tilting-angle-dependent oscillation frequency extracted from the FFT analysis of curves in (b). The red curve is the $1/\cos\theta$ fitting.

II. EXPERIMENTAL DETAILS

In this work, single crystals of $ZrTe_5$ were grown by chemical vapor transport method with iodine (I_2) as the transport agent similar to our report [25]. Firstly, $ZrTe_5$ polycrystalline samples were synthesized by a direct stoichiometric solid-state reaction in the sealed evacuated quartz tube ($P \sim 4 \times 10^{-6}$ Torr) (at about 773 K for 7 days) with highly pure Zr (GRINM, 99.999%) and Te powders (Alfa Aesar, 99.999%) as raw materials. Secondly, the mixture of prepared $ZrTe_5$ polycrystalline and I_2 (about 5 mg/L) powders were ground and loaded into another sealed quartz tube, and then put into a two-zone furnace with a temperature profile of 823–723 K to produce crystals. Finally, the centimeter-level $ZrTe_5$ crystals [shown in Fig. 1(a)] with metallic luster were obtained successfully after growing for over 10 days. The growth orientation of the polished crystals was investigated by single-crystal x-ray diffraction (XRD) measurement using an x-ray diffractometer (Ultima III Rigaku) using Cu-Kα radiation with 2θ of 10 $\sim$ 70°. A transmission electron microscope (TEM, Tecnai-F20, FEI Inc.) operated at 200 kV was applied to microstructure of the $ZrTe_5$ samples. In detail, the samples were ground and then some foils were dispersed in the copper grids with supporting carbon films to carry out TEM measurement. Standard four-probe method was employed on the rectangular $ZrTe_5$ crystals at cryogenic temperatures to measure the electrical transport properties using a 9-T physical properties measurement system (PPMS-9 T, Quantum Design). During the measurements, the electrical current is aligned along the [100] direction and the electrodes covered the whole samples to avoid the current-injecting effect [26].

III. RESULTS AND DISCUSSION

Bulk $ZrTe_5$ takes the orthorhombic layered structure wherein $ZrTe_5$ monolayers stack along the b axis as shown in Fig. 1(a) [7]. In each monolayer $ZrTe_5$, $ZrTe_3$ chains are linked via Te_2 zigzag chains along the c axis. The optical micrograph of the grown $ZrTe_5$ single crystals is depicted in Fig. 1(b) and it shows that the grown $ZrTe_5$ crystals are as large as $30 \times 5 \times 0.5\,\mathrm{mm}^3$. The crystal orientations can be determined by XRD. Figure 1(c) shows the XRD result measured on the exposed surface. All the peaks can be indexed as (0 k 0) reflections of $ZrTe_5$ crystals. It substantiates that the exposed surface of $ZrTe_5$ crystals belongs to b plane. Using the same method, the c plane is also determined by x-ray diffraction. The high-resolution TEM and the corresponding selected area electron diffraction images, taken with electron beam aligned along the [100] axis of $ZrTe_5$, are shown in Fig. 1(d) and its inset. These structural characterizations verify that our grown $ZrTe_5$ crystals have *single-crystalline* quality.

The temperature dependence of longitudinal resistances (shown in Supplemental Material [27]) of $ZrTe_5$ crystals from 2 to 300 K under variable B have an abnormal resistivity maximum around 150 K, which is the same as those reported previously [8–10]. Hereafter we are mainly focused on the study of topological character of $ZrTe_5$ at 2 K through SdH quantum oscillation.

The B-dependent magnetoresistance under tilted angle was measured at 2 K in both b- and c plane. Obviously, the oscillations up to eighth order can be observed on SdH oscillation of both b- and c-plane $ZrTe_5$ under maximum $B \sim 9$ T, which suggests that our $ZrTe_5$ crystals have unprecedented crystalline quality. In b plane, the SdH oscillation is revealed at tilted angles θ, where θ is defined as the angle between B and the b axis [see the inset of Fig. 2(a)]. To clarify the relationship between these curves, Fig. 2(c) plots the angle-dependent oscillation frequencies S_F extracted from the fast Fourier transform (FFT) of the oscillation part in magnetoresistance B curves. The value of oscillation frequencies can be well fitted

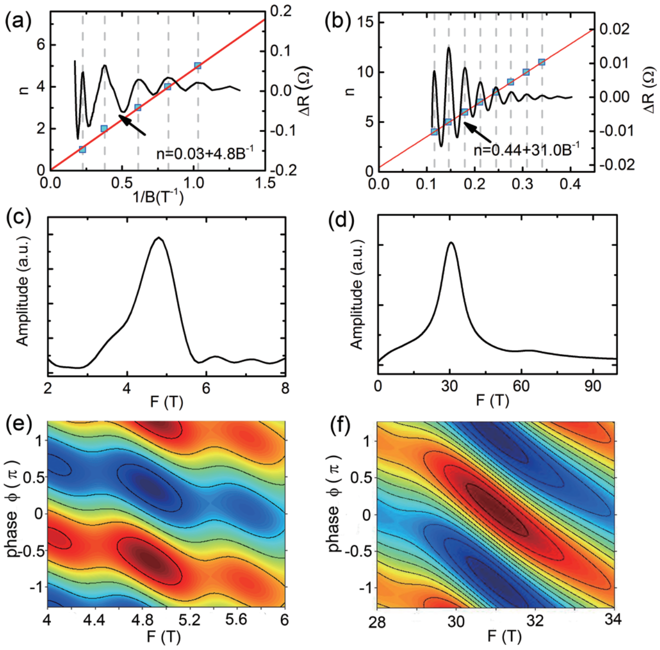

FIG. 3. (a), (b) Curves of $\Delta\rho_{xx}$ vs $1/B$ on b- and c plane are plotted after subtracting a smooth background, respectively, and the corresponding Landau-level fan diagrams for SdH oscillations in b- and c plane. Linear fitting of the periodic resistivity maxima $\Delta\rho_{xx}$ as a function of the Landau-level index n gives a nonzero intercept of 0.03 ± 0.01 for b plane, but intercept for c-plane SdH oscillation is 0.44 ± 0.01. It suggests that there is π-Berry phase in c-plane SdH oscillation, rather than b-plane SdH oscillation. (c), (d) The major oscillation frequency $F = 4.8$ T and $F = 31.0$ T obtained from the FFT are shown for b- and c plane, respectively. (e), (f) Contour plot of the phase-shift function $K(\varphi,B)$ in the vicinity of the SdH oscillation peaks for b- and c plane, respectively. Berry phase on c-plane SdH oscillation extracted from phase-shift function is $(0.95 \pm 0.04)\pi$.

with the relationship $1/\cos\theta$ [28–32] at low tilting angles ($<60°$) and one can see the obvious deviation at high tilting angles ($>60°$). It suggests that SdH oscillation on b plane could be due to either the bulk electron with long ellipsoid Fermi surface topology [10] or nontrivial surface state [31,32]. Using the same method, the titled B-dependent magnetoresistance in the c plane is plotted in Figs. 2(b) and 2(d), where tilting angle θ is redefined as the angle between B and c axis [see the inset of Fig. 2(b)]. The SdH oscillations are also observed at varied angles. The value of the oscillation frequencies S_F can also be well fitted by the relationship $1/\cos\theta$ [32] at low tilting angles ($<60°$). It thus suggests that quasi-two dimensional (quasi-2D) character also exists in the c plane of $ZrTe_5$ crystal, but it still cannot determine the topological property of $ZrTe_5$ crystals.

Because quasi-2D Fermi surfaces are found in both b- and c plane, we may think that $ZrTe_5$ belongs to strong topological insulator or Dirac semimetal. But, the most crucial criterion to distinguish the nontrivial surface state (Dirac fermion) from quasi-two-dimensional bulk electron (Schrödinger fermion) is the π-Berry phase [7,32]. Below, we extract the phase factor of the SdH oscillations. After subtracting a smooth background, Figs. 3(a) and 3(b) show the oscillatory component of ΔR_{xx} vs $1/B$ at 2 K for b- and c plane, respectively. Because the longitudinal resistivity ρ_{xx} is larger than the transverse one $\rho_{xy}(\rho_{xx} : \rho_{xy} \sim 5)$ in our $ZrTe_5$ samples, conductivity σ_{xx} can be approximated to $1/\rho_{xx}$. According to the Lifshitz-Kosevich formula used to extract phase information in topological insulators [32], the quantum oscillation of conductivity can be written as

$$\Delta\sigma \propto \cos\left[2\pi\left(\frac{F}{B} - \frac{1}{2} + \frac{\phi_B}{2\pi} + \delta\right)\right], \quad (1)$$

where F and ϕ_B are oscillation frequency and Berry phase, respectively. δ is the additional phase shift that is within range of -0.125 to 0.125 dependent on dimensionality of the Fermi surface. To simplify the following discussion, we defined phase shift $\phi = 2\pi(-\frac{1}{2} + \frac{\phi_B}{2\pi} + \delta)$ that can be directly extracted by fast Fourier transformation. By means of Eq. (1), we take the linear fitting of the periodic *resistivity maximum* (equivalent to conductivity minimum) as a function of the Landau index N. In this condition, magnetic field B_N should be satisfied:

$$2\pi\left(\frac{F}{B_N} - \frac{1}{2} + \frac{\phi_B}{2\pi} + \delta\right) = 2\pi\left(N - \frac{1}{2}\right). \quad (2)$$

The corresponding Landau fan diagrams ($\frac{1}{B_N} - N$) for b- and c-plane SdH oscillation of $ZrTe_5$ crystal are shown in Figs. 3(a) and 3(b), respectively. The intercepts of b- and c-plane SdH oscillation of $ZrTe_5$ are 0.03 and 0.44, respectively. In accordance with Eq. (2), the Berry phase ϕ_B for b- and c-plane SdH oscillation are 0.06π and 0.88π, respectively. In other words, electrons leading to SdH oscillation at b- and c plane belong to Schrödinger fermion (bulk state) and Dirac fermion (surface state), respectively.

To cross check the Landau fan analysis, phase-shift analysis was conducted [33,34]. Firstly, the SdH oscillation result was Fourier-transformed and then the phase-shift function was plotted, where phase-shift function K is defined as $K(\varphi,B) = \mathrm{Re}\{e^{-i\varphi} f(B)\}$, and $f(B)$ is the complex Fourier transformation of the low magnetic field magnetoresistance ΔR_{xx}. More technical details of phase-shift analysis can be found in Refs. [33,34]. The oscillation frequency and phase shift thus can be extracted from the maximum of phase-shift function $K(\varphi,B)$. The pictures of phase-shift function for b- and c-plane SdH oscillation are shown in Figs. 3(e) and 3(f), respectively. One can see the major oscillation frequencies $F = 4.8$ T and $F = 31.0$ T for b- and c planes [Figs. 4(c) and 4(d)], respectively. These values are quite similar to those reported previously [9,10]. As shown in Figs. 3(e) and 3(f), the phase shifts in the b- and c-plane SdH oscillation are $-(0.64 \pm 0.02)\pi$ and $(0.05 \pm 0.02)\pi$, respectively. According to the definition of phase shift $\phi = 2\pi(-\frac{1}{2} + \frac{\phi_B}{2\pi} + \delta)$, Berry phase ϕ_B of b- and c-plane SdH quantum oscillation can be determined as $(0.16 \pm 0.04)\pi$ and $(0.95 \pm 0.04)\pi$ by assuming $\delta \sim 0.1$, respectively. This conclusion is quite close to analysis by Landau fan diagram.

Finally, we would like to point out the origin of the 2D-like $1/\cos(\theta)$-S_F feature observed in b-plane $ZrTe_5$ [Fig. 2(c)]. Figures 4(a) and 4(b) show the energy-band structure of $ZrTe_5$ in weak TI state and corresponding Fermi surface of bulk electron, respectively. It should be mentioned that the theoretical band structure and Fermi surface shown in Fig. 4 are quite similar to the experimental ARPES results [22–24]. The Fermi level is determined through comparison

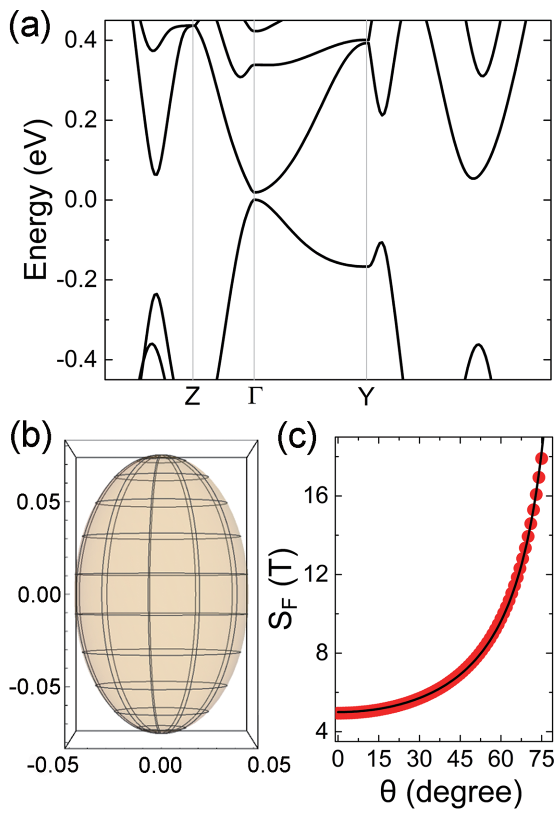

FIG. 4. (a) Bulk electronic band structure of $ZrTe_5$ in the weak topological insulator state. (b) Fermi surface of bulk electron of $ZrTe_5$; the Fermi surface is determined by comparison of the maximum cross section of Fermi surface at $K_b = 0$ with the experimental one determined by b-axis SdH oscillation. The scale is enlarged ten times to visualize clearly. (c) The dependence of theoretical S_F on tilting angle θ. Red dots are theoretical data, black line is fitting of $S_F \sim 1/\cos(\theta)$. Obviously, it is in agreement with experimental observation [Fig. 2(c)].

between the theoretical maximum cross section (S_M) and the experimental one along the b axis. Evidently, bulk Fermi surface of $ZrTe_5$ along the b axis is like a long ellipse. The dependence of theoretical S_F on tilting angle θ is depicted at Fig. 4(c). Obviously, the θ-dependent S_F can be fitted to the $1/\cos(\theta)$ relationship, which is in agreement with experimental observation [see Fig. 2(c)]. Therefore, it verifies that the 2D-like $1/\cos(\theta)$-S_F feature observed in b-plane $ZrTe_5$ comes from bulk electrons.

Based on the above-mentioned analysis, we would like to discuss the topological phase of bulk $ZrTe_5$ at 2 K. The possible electronic states of $ZrTe_5$ are normal narrow-gap semiconductor, Dirac semimetal, and strong and weak topological insulator. Normal narrow-gap semiconductor can be ruled out because of the existence of a nontrivial Berry phase on c plane. Dirac semimetal and strong topological insulator might be impossible too, because there are nontrivial surface states on all six-surface crystal, like those observed in the prototypical strong topological insulator-Bi_2Se_3 material systems [32]. In other words, the SdH oscillations in all six-surface should have a nontrivial π-Berry phase. Therefore, the most possible candidate is the weak topological insulator (WTI). In the WTI state, there are only four surfaces (a- and c planes) of $ZrTe_5$ crystal hosted 2D Dirac fermion that have the nontrivial π-Berry phase, which is in agreement with our experimental observation (see Fig. 3). Another fingerprint of weak topological insulator of $ZrTe_5$ is the existence of electronic band gap at b plane, which is clearly seen in Fig. S2 [27].

IV. CONCLUSION

In summary, we synthesized the high-quality $ZrTe_5$ crystals and systematically characterized the quantum oscillations in the b- and c plane of $ZrTe_5$ single crystals under tilted B at 2 K. Detailed Berry-phase determination, as well as comparison between experimental and theoretical fermiology features, verify that SdH oscillation at b plane comes from bulk electrons with long ellipse Fermi surface, while that at c plane does from surface electrons with nontrivial π-Berry phase. These results strongly suggest that bulk $ZrTe_5$ at 2 K is a weak topological insulator rather than a 3D Dirac semimetal or a strongly topological insulator reported previously. This work is helpful to resolve the current debate on the topological property of bulk $ZrTe_5$.

ACKNOWLEDGMENTS

We would like to acknowledge the financial support from the National Natural Science Foundation of China (Grants No. 51472112, No. 51032003, No. 11374140, No. 11374149, No. 11004094, No. 11134006, and No. 11174127), and State Key Program for Basic Research of China (973 Program) (Grants No. 2015CB921203 and No. 2013CB922103). Y.-Y.L. acknowledges the financial support from the program A for Outstanding PhD candidate of Nanjing University. Y.B.C. wishes to express sincere thanks to Prof. H. M. Weng and Prof. L. Lu at Institute of Physics for their enlightening discussions, T. Y. Zhao for his work on Fig. 4, as well as Prof. D. K. Maude for sharing with us his code on phase-shift function, and enlightening discussion.

Y.-Y.L. and B.-B.Z. contributed equally to this work.

[1] C. L. Kane and E. J. Mele, Quantum Spin Hall Effect in Graphene, Phys. Rev. Lett. **95**, 226801 (2005).

[2] B. A. Bernevig, T. L. Hughes, and S. C. Zhang, Quantum spin Hall effect and topological phase transition in HgTe quantum wells, Science **314**, 1757 (2006).

[3] M. König, S. Wiedmann, C. Brüne, A. Roth, H. Buhmann, L. W. Molenkamp, X.-L. Qi, and S.-C. Zhang, Quantum spin Hall insulator state in HgTe quantum wells, Science **318**, 766 (2007).

[4] I. Knez, R.-R. Du, and G. Sullivan, Evidence for Helical Edge Modes in Inverted InAs/GaSb Quantum Wells, Phys. Rev. Lett. **107**, 136603 (2011).

[5] X. F. Qian, J. W. Liu, L. Fu, and J. Li, Quantum spin Hall effect in two-dimensional transition metal dichalcogenides, Science **346**, 1344 (2014).

[6] H. J. Zhang, Y. Xu, J. Wang, K. Chang, and S. C. Zhang, Quantum Spin Hall And Quantum Anomalous Hall States Realized in Junction Quantum Wells, Phys. Rev. Lett. **112**, 216803 (2014).

[7] H. M. Weng, X. Dai, and Z. Fang, Transition-Metal Pentatelluride $ZrTe_5$ and $HfTe_5$: A Paradigm For Large-Gap Quantum Spin Hall Insulators, Phys. Rev. X **4**, 011002 (2014).

[8] F. J. DiSalvo, R. M. Fleming, and J. V. Waszczak, Possible phase transition in the quasi-one-dimensional materials $ZrTe_5$ or $HfTe_5$, Phys. Rev. B **24**, 2935 (1981).

[9] M. Izumi, K. Uchinokura, R. Yoshizaki, S. Harada, T. Nakayama, A. Yamada, and E. Matsuura, Transport properties and Fermi surfaces in $HfTe_5$ and $ZrTe_5$, J. Phys. Colloques **44**, C3-1705 (1983).

[10] G. N. Kamm, D. J. Gillespie, A. C. Ehrlich, and T. J. Wieting, Fermi surface, effective masses, and Dingle temperatures of $ZrTe_5$ as derived from the Shubnikov-de Haas effect, Phys. Rev. B **31**, 7617 (1985).

[11] M. Izumi, T. Nakayama, K. Uchinokura, S. Harada, R. Yoshizaki, and E. Matsuura, Shubnikov-de Haas oscillations and Fermi surfaces in transition-metal pentatellurides $ZrTe_5$ and $HfTe_5$, J. Phys. C: Solid State Phys. **20**, 3691 (1987).

[12] T. M. Tritt, N. D. Lowhorn, R. T. Littleton IV, A. Pope, C. R. Feger, and J. W. Kolis, Large enhancement of the resistive anomaly in the pentatelluride materials $HfTe_5$ and $ZrTe_5$ with applied magnetic field, Phys. Rev. B **60**, 7816 (1999).

[13] Q. Li, D. E. Kharzeev, C. Zhang, Y. Huang, I. Pletikosic, A. V. Fedorov, R. D. Zhong, J. A. Schneeloch, G. D. Gu, and T. Valla, Chiral magnetic effect in $ZrTe_5$, Nat. Phys. **12**, 550 (2016).

[14] R. Y. Chen, S. J. Zhang, J. A. Schneeloch, C. Zhang, Q. Li, G. D. Gu, and N. L. Wang, Optical spectroscopy study of the three-dimensional Dirac semimetal $ZrTe_5$, Phys. Rev. B **92**, 075107 (2015).

[15] R. Y. Chen, Z. G. Chen, X.-Y. Song, J. A. Schneeloch, G. D. Gu, F. Wang, and N. L. Wang, Magnetoinfrared Spectroscopy of Landau Levels and Zeeman Splitting of Three-Dimensional Massless Dirac Fermions in $ZrTe_5$, Phys. Rev. Lett. **115**, 176404 (2015).

[16] G. L. Zheng, J. W. Lu, X. D. Zhu, W. Ning, Y. Y. Han, H. W. Zhang, J. L. Zhang, C. Y. Xi, J. Y. Yang, H. F. Du, K. Yang, Y. Z. Zhang, and M. L. Tian, Transport evidence for the three-dimensional Dirac semimetal phase in $ZrTe_5$, Phys. Rev. B **93**, 115414 (2016).

[17] X. Yuan, C. Zhang, Y. W. Liu, A. Narayan, C. Y. Song, S. D. Shen, X. Sui, J. Xu, H. C. Yu, Z. H. An, J. Zhao, S. Sanvito, H. G. Yan, and F. X. Xiu, Observation of quasi-two-dimensional Dirac fermions in $ZrTe_5$, NPG Asia Mater. **8**, e325 (2016).

[18] Y. W. Liu, X. Yuan, C. Zhang, Z. Jin, A. Narayan, C. Luo, Z. G. Chen, L. Yang, J. Zou, X. Wu, S. Sanvito, Z. C. Xia, L. Li, Z. Wang, and F. X. Xiu, Zeeman splitting and dynamical mass generation in Dirac semimetal $ZrTe_5$, Nat. Commun. **7**, 12516 (2016).

[19] G. Manzoni, A. Sterzi, A. Crepaldi, M. Diego, F. Cilento, M. Zacchigna, Ph. Bugnon, H. Berger, A. Magrez, M. Grioni, and F. Parmigiani, Ultrafast Optical Control of the Electronic Properties of $ZrTe_5$, Phys. Rev. Lett. **115**, 207402 (2015).

[20] X.-B. Li, W.-K. Huang, Y.-Y. Lv, K.-W. Zhang, C.-L. Yang, B.-B. Zhang, Y. B. Chen, S.-H. Yao, J. Zhou, M.-H. Lu, L. Sheng, S.-C. Li, J.-F. Jia, Q.-K. Xue, Y.-F. Chen, and D.-Y. Xing, Experimental Observation of Topological Edge States at the Surface Step Edge of the Topological Insulator $ZrTe_5$, Phys. Rev. Lett. **116**, 176803 (2016).

[21] R. Wu, J.-Z. Ma, S.-M. Nie, L.-X. Zhao, X. Huang, J.-X. Yin, B.-B. Fu, P. Richard, G.-F. Chen, Z. Fang, X. Dai, H.-M. Weng, T. Qian, H. Ding, and S. H. Pan, Evidence for Topological Edge States in a Large Energy Gap Near the Step Edges on the Surface of $ZrTe_5$, Phys. Rev. X **6**, 021017 (2016).

[22] L. Moreschini, J. C. Johannsen, H. Berger, J. Denlinger, C. Jozwiak, E. Rotenberg, K. S. Kim, A. Bostwick, and M. Grioni, Nature and topology of the low-energy states in $ZrTe_5$, Phys. Rev. B **94**, 081101(R) (2016).

[23] H. Xiong, J. A. Sobota, S.-L. Yang, H. Soifer, A. Gauthier, M.-H. Lu, Y.-Y. Lv, S.-H. Yao, D. Lu, M. Hashimoto, P. S. Kirchmann, Y.-F. Chen, and Z.-X. Shen, Three-dimensional nature of the band structure of $ZrTe_5$ measured by high-momentum-resolution photoemission spectroscopy, Phys. Rev. B **95**, 195119 (2017).

[24] Y. Zhang, C. L. Wang, L. Yu, G. D. Liu, A. J. Liang, J. W. Huang, S. M. Nie, X. Sun, Y. X. Zhang, B. Shen, J. Liu, H. M. Weng, L. X. Zhao, G. F. Chen, X. W. Jia, C. Hu, Y. Ding, W. J. Zhao, Q. Gao, C. Li, S. L. He, L. Zhao, F. F. Zhang, S. J. Zhang, F. Yang, Z. M. Wang, Q. J. Peng, X. Dai, Z. Fang, Z. Y. Xu, C. T. Chen, and X. J. Zhou, Electronic evidence of temperature-induced Lifshitz transition and topological nature in $ZrTe_5$, Nat. Commun. **8**, 15512 (2017).

[25] Y.-Y. Lv, F. Zhang, B.-B. Zhang, B. Pang, S.-H. Yao, Y. B. Chen, L. W. Ye, J. Zhou, S.-T. Zhang, and Y.-F. Chen, Microstructure, growth mechanism and anisotropic resistivity of quasi-one-dimensional $ZrTe_5$ crystal, J. Cryst. Growth **457**, 250 (2017).

[26] C.-L. Zhang, S.-Y. Xu, I. Belopolski, Z. J. Yuan, Z. Q. Lin, B. B. Tong, G. Bian, N. Alidoust, C.-C. Lee, S.-M. Huang, T.-R. Chang, G. Q. Chang, C.-H. Hsu, H.-T. Jeng, M. Neupane, D. S. Sanchez, H. Zheng, J. F. Wang, H. Lin, C. Zhang, H.-Z. Lu, S.-Q. Shen, T. Neupert, M. Z. Hasan, and S. Jia, Signatures of the Adler-Bell-Jackiw chiral anomaly in a Weyl fermion semimetal, Nat. Commun. **7**, 10735 (2016).

[27] See Supplemental Material at http://link.aps.org/supplemental/10.1103/PhysRevB.97.115137 for the detailed analysis.

[28] F. X. Wu, J. Zhou, L. Y. Zhang, Y. B. Chen, S.-T. Zhang, Z.-B. Gu, S.-H. Yao, and Y.-F. Chen, Metal-insulator transition in $SrIrO_3$ with strong spin-orbit interaction, J. Phys.: Condens. Matter. **25**, 125604 (2013).

[29] D. X. Qu, Y. S. Hor, J. Xiong, R. J. Cava, and N. P. Ong, Quantum oscillations and Hall anomaly of surface states in the topological insulator Bi_2Te_3, Science **329**, 821 (2010).

[30] A. A. Taskin, Z. Ren, S. Sasaki, K. Segawa, and Y. Ando, Observation of Dirac Holes and Electrons in a Topological Insulator, Phys. Rev. Lett. **107**, 016801 (2011).

[31] Z. Ren, A. A. Taskin, S. Sasaki, K. Segawa, and Y. Ando, Large bulk resistivity and surface quantum oscillations in the topological insulator Bi_2Te_2Se, Phys. Rev. B **82**, 241306(R) (2010).

[32] Y. Ando, Topological insulator materials, J. Phys. Soc. Jpn. **82**, 102001 (2013).

[33] I. A. Luk'yanchuk and Y. Kopelevich, Phase Analysis of Quantum Oscillations in Graphite, Phys. Rev. Lett. **93**, 166402 (2004).

[34] J. M. Schneider, M. Orlita, M. Potemski, and D. K. Maude, Consistent Interpretation of the Low-Temperature Magnetotransport in Graphite Using the Slonczewski-Weiss-McClure 3D Band-Structure Calculations, Phys. Rev. Lett. **102**, 166403 (2009).